Published in final edited form as:
Chem Biol. 2013 July 25; 20(7): 956–967. doi:10.1016/j.chembiol.2013.06.005.

Phenotypic Assays For β-Amyloid In Mouse Embryonic Stem Cell-derived Neurons

Laura Beth J. McIntire[1], **Natalie Landman**[1,2], **Min Suk Kang**[1], **Gina Finan**[1], **Jeremy Hwang**[3], **Ann Z. Moore**[4], **Lydia S. Park**[1], **Chyuan-Sheng Lin**[5], and **Tae-Wan Kim**[1,*]

[1]Department of Pathology and Cell Biology, and the Taub Institute for Research on Alzheimer's Disease and the Aging Brain, Columbia University Medical Center, New York, NY10032, USA

[5]Irving Cancer Research Center, Columbia University Medical Center, New York, NY10032, USA

SUMMARY

Given the complex nature of Alzheimer's disease (AD), a cell-based model that recapitulates physiological properties of the target neuronal population carries significant value in discovering improved drug candidates and chemical probes for uncovering disease mechanisms. We established phenotypic neuronal assays for biogenesis and synaptic action of amyloid β-peptide (Aβ) based on embryonic stem (ES) cell-derived neurons (ESNs). ESNs enriched with pyramidal neurons were robust, scalable and amenable to a small molecule screening assay, overcoming apparent limitations of neuronal models derived from human pluripotent cells. Small molecule screening of clinical compounds identified four compounds capable of reducing Aβ levels in ESNs derived from the Tg2576 mouse model of AD. Our approach is therefore highly suitable for phenotypic screening in AD drug discovery and has the potential to identify therapeutic candidates with improved efficacy and safety potential.

INTRODUCTION

Elevation and accumulation of amyloid β-peptide (Aβ) in brain are early and necessary steps in pathogenesis of Alzheimer's disease (AD), preceding all known clinical and pathological phenotypes of the disease, including memory and cognitive decline, by at least a decade (Hardy and Selkoe, 2002; O'Brien and Wong, 2011; Zheng and Koo, 2011). Aβ is liberated from β-amyloid precursor protein (APP) by membrane-bound proteases, β-secretase (BACE1) and γ-secretase (Hardy and Selkoe, 2002; O'Brien and Wong, 2011; Zheng and Koo, 2011). The majority of current therapeutic strategies have focused on developing potent small molecule inhibitors for targeting well-defined enzymatic targets, including the secretase enzymes. Despite initial promise, the majority of these approaches suffered major setbacks in late stage clinical trials (Mangialasche, 2010). Therefore, model systems and biomarkers that can better predict the efficacy and safety of therapeutic candidates in human clinical trials have become increasingly important.

*Corresponding author: Dr. Tae-Wan Kim, address: Department of Pathology and Cell Biology, Columbia University Medical Center, 630 West 168th Street, P&S 12-430, New York, NY 10032, USA, phone: 212-305-5786; fax: 212-342-1839, twk16@columbia.edu.
[2]Present address: Healthcare Transformation Institute, Arizona State University, Phoenix, AZ85259, USA
[3]Present address: Doheny Eye Institute, Los Angeles, CA90089, USA
[4]Present address: Translational Gerontology Branch, National Institute on Aging, Baltimore, MD21225, USA

Cell types historically used in AD drug discovery, such as immortalized or genetically transformed neuronal lines, lack complete phenotypic properties of primary neurons. Dissociated primary neuronal cultures, though a better physiological model compared to cell lines, have major limitations due to survival time in culture, cellular heterogeneity and inability for large scale production (McNeish, 2004; Pouton and Haynes, 2007). Stem cell technology furnishes a novel opportunity for the generation of a physiologically relevant disease model using directed differentiation of stem cells into the optimal model cell type suitable for functional study and drug discovery (McNeish, 2004; Pouton and Haynes, 2007; Rubin and Haston, 2011).

Creation of a human neuronal model derived from human embryonic stem (ES) cells or patient-derived induced pluripotent stem (iPS) cells would ultimately serve as the ideal disease model, eventually able to predict drug responsiveness in cells originating from the patient's own tissue (Yamanaka and Blau, 2010; Jang et al., 2012) However, despite great promise, productive and reliable use of human ES or iPS cells in drug discovery remains challenging (Ebert and Svendsen, 2010; Han et al., 2011). For drug screening applications such as high throughput screening (HTS), human ES and iPS protocols require laborious maintenance which make automation and differentiation into functional neurons challenging (Ebert and Svendsen, 2010). Furthermore, genetic and epigenetic variability among patients may influence pharmacological responsiveness, hindering the practical application of stem cells from human patient origin for drug discovery (Han et al, 2011). In contrast to human stem cells, mouse ES (mES) cells harbor several notable advantages for bioassays and drug discovery applications, including the relatively homogenous nature of differentiated cells, potential derivation from disease models and convenient expandability (Pouton and Haynes, 2007). It has been shown that mES cells can be differentiated into specific neuronal subtype(s), including pyramidal neurons, a significantly vulnerable neuronal population in AD (Mann, 1996; Morrison and Hof, 2002).

To establish an AD-centric primary neuronal model, we developed phenotypic cell-based assays for the biogenesis and synaptic action of Aβ using mouse ES cell-derived neuronal cultures enriched in functional pyramidal neurons. We isolated ES cells from a mouse model of the disease, Tg2576 which harbors human APP with the Swedish mutation (APP_{sw}). To validate application of mouse embryonic stem cell-derived neurons (ESNs) we screened a library of clinical compounds and identified four compounds capable of reducing Aβ levels. Our neuronal model is therefore highly suitable for phenotypic screening in AD drug discovery and has the potential to enhance the predictive value of cell-based screening assays for lead compounds with a higher probability of surviving advanced rounds of vetting for efficacy and diminished toxicity.

RESULTS

Characterization of Pyramidal Cell Enriched ESN Cultures

A neuronal culture highly enriched in pyramidal neurons was produced by directed differentiation of mES cells by modifying published protocols (Figure 1A) (Bibel et al., 2004; Bibel et al., 2007). Neuronal morphology was apparent after 1 day *in vitro* (DIV) and the majority of cells displayed neuronal morphology by DIV 5 (Figure 1A). By DIV 7 neuronal proteins including neuronal β-tubulin III (TUJ-1) and pyramidal neuron marker EMX1 were expressed indicating a highly homogenous neuronal population enriched in pyramidal neurons (Figures 1B and 1D) (Chan et al., 2001). Glial cells, identified by glial fibrillary acidic protein (GFAP) were only rarely observed (Figures 1C and 1D). Neuron specific proteins, neuronal β-tubulin (TUJ-1) and synaptophysin, as well as glutamatergic neuronal proteins, TrkB and CaMKIIα, increased from DIV 1-7 and there was a gradual decline in the levels of the p75 neurotrophin receptor ($p75^{NTR}$) consistent with maturing

pyramidal neurons (Figure 1E) (Buck et al., 1988). The subcellular distribution of endogenous pre-synaptic synaptophysin and post-synaptic PSD-95 as adjacent puncta along dendrites recapitulated mature synapses in primary neurons (Figure 1F). Electron microscopy (EM) analysis revealed that both presynaptic vesicles as well as postsynaptic densities were apparent in this culture (Figure 1G). Expression of PSD-95 and synaptophysin was evident by Western analysis by DIV 14 (Figure 1H).

Modeling Aβ-induced synaptic alterations in ESNs

Oligomeric Aβ induces both structural and functional alterations at synapses in cultured neurons (Pozueta et al., 2012). To model this using mouse ESNs, we examined the effects of Aβ treatment on synaptic morphology and changes in cell signaling events indicative of synaptic plasticity. Synapse loss is documented in AD mouse models and after treatment of neurons with oligomeric Aβ, correlating with the loss of immunoreactivity of PSD-95, a postsynaptic protein (Gylys et al., 2004; Roselli et al., 2005; Cerpa et al., 2010). In ESNs, oligomeric Aβ treatment decreased PSD-95 puncta count, fractional area and total area but synaptophysin puncta, a presynaptic protein, remained unchanged (Figures 2A-2F) (Hu, et al., 2003; King ad Arendash, 2002; Jacobsen et al.,2006). Aβ treatment also triggers morphological defects in synaptic spines including reduction in dendritic spine density (Hsieh et al., 2006; Shankar et al., 2007; Lacor et al.,2007). Diolistic labeling of neurons (Moolman et al., 2004; McIntire et al., 2012) revealed that treatment of ESNs with Aβ oligomers reduced spine density (Figure 2G, H). After Aβ oligomer treatment, spine length increased modestly and slightly decreased dendritic diameter (Figures 2I and 2J) (Calabrese et al., 2007; Lacor et al., 2007). In addition to morphological spine changes, at a functional level, Aβ has been shown to induce characteristic molecular changes in neurons, including suppressed phosphorylation of cyclic AMP response element binding protein, CREB, a memory-associated transcription factor (Vitolo et al., 2002; Snyder et al., 2005). In ESNs, Aβ oligomer treatment prevented NMDA stimulation dependent phosphorylation of CREB (pCREB) (Figures 2K and 2L). Treatment of ESNs with Aβ oligomer at high concentrations led to neuronal death (Figure S1).

Expression of Secretase Components in ESNs

To determine if ESNs would effectively model Aβ biogenesis, we determined expression of enzymatic components of APP processing. ESNs express the β-site APP cleaving enzyme (BACE1) at later stages of differentiation but not in ES cells (Figures 3A and 3C) (O'Brien and Wong, 2011; Zheng and Koo, 2011). In contrast, PS1 was detected in mES cells consistent with its described role in development (Figure 3B) (Wong et al., 1997). Further, APP and BACE1 were enriched in the late endosomal compartment enriched for syn6 and rab11 and de-enriched in early endosomes containing early endosomal protein A1 (EEA1) consistent with published distribution in cultured primary neurons (Figure 3C) (Tang, 2009; Finan et al., 2011; Wen et al., 2011).

Genetic Modeling of Expression of FAD-associated APP and PS1 in ESNs

To model familial AD (FAD), wild type ESNs were infected with APP_{sw} lentivirus and APP processing was analyzed. Treatment of infected ESNs with BACE1 inhibitor (BSI) (Stachel, 2006) reduced secretion of sAPPβ, Aβ40 and Aβ42 while treatment with γ-secretase inhibitor (GSI) (Seiffert, 2000) inhibited Aβ40 and Aβ42 secretion without affecting the levels of secreted APP β-cleaved fragment (sAPPβ) or secreted APP α-cleaved fragment (sAPPα) (Figures 3D and 3F). Consistent with previous studies in cell models and mouse brain, C-terminal fragments (CTFs) resulting from APP cleavage, accumulated in response to GSI treatment (Figure 3D) (Hardy and Selkoe, 2002; O'Brien and Wong, 2011; Zheng and Koo, 2011; Landman et al., 2006; Okada et al., 2010).

To model PS1-linked FAD phenotypes in ESNs, three different FAD mutant PS1 transgenes (ΔE9, M146V, and L286V) were elctroporated into mES cells to produce ES lines stably expressing the mutants. Resulting stable mES cells were subjected to directed differentiation into pyramidal neurons. A representative Western blot shows the PS1 transgene and normal neuronal protein expression in ESNs derived from these clonal mES cell lines (Figures 3G and 3H). An increase in the Aβ42/ Aβ40 ratio, a key pathogenic phenotype associated with PS1 FAD (O'Brien and Wong, 2011; Zheng and Koo, 2011) was observed in ESNs expressing ΔE9 M146V, and L286V mutant forms of PS1 after APP_{sw} lentiviral infection (Figure 3I).

ESNs from Tg2576 Mouse Model of AD

In order to achieve robust and reproducible neuronal expression of human APP, mES cells were isolated from the inner cell mass of blastocysts from a well characterized mouse model of AD, Tg2576 (Hsiao et al., 1996). ESNs from Tg2576 showed normal neuronal differentiation by morphology and neuronal protein expression (Figures 4A and 4B), comparable to neuronal differentiation of wild-type ES cells. Transgene-derived human APP_{sw} was expressed at DIV 1-7, but little expression was detected in the undifferentiated mES cells (Figure 4B). APP processing at DIV 7 was sensitive to BSI, GSI and an α–secretase inhibitor, TAPI-2. APP CTF expression increased in response to GSI treatment, but levels of neuronal proteins synaptophysin, CaMKIIα and neuronal β-tubulin did not change with any pharmacological treatment (Figure 4C). Soluble sAPPα and sAPPβ were reduced by TAPI-2 and BSI treatment respectively (Figure 4D). Further, human Aβ40 and Aβ42 were reduced by treatment of neurons with BSI and GSI as predicted (Figures 4E and 4F) (Stachel, 2006; Seiffert, 2000).

High Throughput Screening Assay for Aβ in Tg2576 ESNs

High-throughput screening (HTS) using a miniaturized assay allows rapid and parallel examination of the bioactivities of large numbers of compounds. To accommodate HTS in ESNs, we miniaturized an Aβ detection assay using Tg2576 ESNs cultured in a 96 multi-well plate. We determined the optimal cell density and assay parameters to optimize suitability and robustness for HTS application. The optimal cell density of 1.5×10^5 cells/cm^2 maximized the cell viability signal (Figures 5A and 5C). Two parameters commonly used to evaluate the robustness of a HTS assay are the coefficient of variance (%CV) and Z' factor (Inglese et al., 2007). Typically, an assay with %CV value <15% and Z' factor >0.5 is considered a robust assay suitable for HTS (Inglese et al., 2007). At the plating density of 1.5×10^5 cells/cm^2, with 5 replicate wells, both the %CV (Figure 5B) and Z' factor (Figure 5C) were optimized. Using the optimized 96 well platform, ESNs derived from the Tg2576 mouse model displayed characteristic inhibitor response kinetic profiles for both BSI and GSI (Figures 4E and 4F) (Stachel, 2006; Seiffert, 2000). Values of %CV for Aβ40 and Aβ42 indicated acceptable variance for signal detection (Inglese et al., 2007). Additional metrics including signal to noise (S:N), signal to background (S:B) and signal window also indicated detection of Aβ40 and Aβ42 was sufficiently higher than variance of the assay (data not shown).

Identification of Clinical Compounds that Reduce Aβ Secretion in ESNs

To fully validate the ESNs-based assay, we screened for inhibitors of Aβ secretion using the NIH clinical collection (NCC) which consists of 446 small molecules that have a history of use in human (Noorbakhsh et al., 2009). Compounds were identified as hits if they reduced Aβ40 by 40% and deviated 4 standard deviations from the average value of negative controls (Figure 6A) but maintained cell viability within 2 standard deviations of control (Figure 6B). The most potent hits identified were amiridine, icariin, phenelzine and progesterone (Figure 6C). The compounds were obtained from an independent source,

activity was confirmed and they were subjected to IC50 determination (Figure 6D). To investigate the possible mechanisms of the Aβ-reducing activity of these compounds, alterations in APP processing were determined in response to compound treatment. Icariin, phenelzine and progesterone reduced sAPPβ levels, suggesting that these compounds may modulate the activity of BACE1 (Figures 6E and 6F). None of the compounds significantly affected levels of sAPPα or full length APP (Figures 6D, 6G and 6H). Aβ40 was confirmed to be reduced by the hit compounds (Figure 6I).

Pharmacological Response of Hit Compounds in ESNs and Cell Lines

An advantage of phenotypic screening in ESNs is the preservation of the cellular context of physiological neurons compared to commonly used cell-based screening assays typically based on transformed cell lines. Therefore, we determined the ability of hit compounds to exert Aβ-lowering activity in APP, PS1 and BACE1 expressing cell lines. Interestingly, icariin, phenelzine and progesterone did not significantly reduce Aβ secretion in any of the three alternate cell lines we tested, including Neuro2a expressing APP_{sw}, CHO expressing APP and mutant PS1 (ΔE9), and SH-SY5Y cells expressing BACE1 and APP (Figure 7). Amiridine reduced Aβ secretion in the SH-SY5Y cell line however, Aβ-reducing activity was not observed in Neuro2a or CHO cell lines (Figure 7).

DISCUSSION

Our current study presents practical applications of mouse ESNs for AD and CNS drug discovery research. ESNs serve as an infinite source of neurons which functionally and morphologically recapitulate pyramidal neurons as well as harbor the appropriate machinery for APP processing and synaptic function. We show that ESNs can be cultured and assayed in a platform suitable for drug screening. Using ESNs from the Tg2576 mouse model of AD, we established and validated a high throughput screening (HTS) platform for an Aβ detection assay and also provided examples of how this platform can be used to probe various key biological and pathophysiological pathways in intact primary neurons, such as analyses of alterations in synaptic function and structure, and APP processing. It is plausible that our ESN platform is also applicable to parallel detection of multiple β-amyloid phenotypes described in this paper, in addition to other AD-associated phenotypes such as tau-associated abnormalities. Thus, to address the complex biological mechanisms underlying AD, our model uniquely permits the investigation of druggable pathways or networks in intact neurons (Noorbakhsh et al., 2009).

The mouse ESN model has appreciably enhanced suitability for HTS compared to human ES and iPS cell-derived neurons. In general, much longer expansion and differentiation periods are required for ESNs and iPS-derived neurons, which typically require 21+ days for differentiation and up to 5 weeks for maturation in culture to display desired phenotypes (Barker, 2012; Dhara and Stice, 2008; Schwartz et al.,2008). Thus, mouse ES cells and ESNs harbor an advantage over human systems for ease of expandability in a practical amount of time for automation (Erceg et al., 2009; Kim et al., 2011; Nistor et al., 2011). Furthermore, it is difficult to obtain relatively homogenous neuronal populations from human pluripoent cells in contrast to mouse ESNs implying that our mouse ESN-based approach is more suitable for quantitative detection and assays owing to relatively homogenous and reproducible neuronal cultures (Engle and Puppala, 2013; Ebert and Svendsen, 2010; Han, 2011) Human iPS cells from AD patients have recently been successfully differentiated into neurons displaying several expected phenotypes including elevated Aβ (Yagi et al., 2011; Israel et al., 2011). However, iPS cell-derived neurons from one sporadic AD patient lacked the Aβ increase altogther, highlighting the inherent variability among patient derived iPS cells due to differences in genetic background compounded with inherent variability among clones from the same patient (Israel et al.,

2011; Choi and Tanzi, 2012; Ooi et al., 2013). Further, since AD has a mixed etiology, selecting appropriate control lines for iPS is challenging considering the variability in genetic background of each patient (Barker, 2012; Choi and Tanzi, 2012). In contrast, mouse ES cell lines can be harvested from the numerous existing mouse models, giving rise to disease models and near-clonal appropriate controls. Genetic and epigenetic integrity in iPS cells may be compromised by insertional defects owing to the integration of ectopic transcription factors (Han et al., 2011; Papp and Plath, 2011). Synapse loss, a critical feature in AD correlating with disease severity, was not observed in recent publications on iPS from AD patients, perhaps due to limited culture duration (Yagi et al., 2011; Choi and Tanzi, 2012), however, mouse ESN display robust synapse formation as well as Aβ-triggered synapse loss (Figure 2). Thus, mouse ESNs uniquely harbor both phenotypic relevance and HTS adaptability. Though mouse ESN are favorable for HTS, human derived ESN and iPS derived neurons currently hold high value for secondary confirmatory studies for compound efficacy and toxicity in the human genetic background.

The four most potent hits identified in our screen are known CNS drugs. Amiridine belongs to the class of aminopyridine acetylcholinesterase inhibitors including tacrine, which have been used in the clinic for the symptomatic treatment for AD (Braginskaya et al., 2001; Yoshida and Suzuki, 1993). An interesting future investigation would be to determine whether the Aβ lowering activity is a common property of all aminopyridine compounds in this drug class and if this activity potentially influences clinical variables. Phenelzine belongs to a class of drugs, the monoamine oxidase inhibitors (MAOI), which have been studied for potential clinical use in AD, based on their ability to promote neurotransmission and improve cognition (Freedman et al., 1998; Mangoni et al., 1991; Sano et al., 1997; Volz and Gleiter, 1998). We found that phenelzine reduced Aβ and sAPPβ secretion suggesting that this compound may reduce Aβ through the inhibition of BACE1 in neurons. In the previous studies, derivatives of this class of drug have been reported to inhibit γ-secretase activity and stimulate sAPPα production in cell lines (Lee et al., 2010; Weinreb et al., 2009; Yodim et al., 2003)., Thus, it is conceivable that phenelzine confers Aβ-reducing activities through multiple mechanisms involving both β- and γ-secretase pathways through cellular target(s) have not yet been identified. Icariin has been reported to reduce Aβ-induced synaptic and cellular deficits (Li et al., 2010; Zeng et al., 2010) and ameliorate memory impairment in Aβ treated rats and a mouse model of AD (Nie et al., 2010; Urano and Tohda, 2010). Icariin has also been reported to reduce the expression of BACE1 (Nie et al., 2010). Consistent with its reported role on BACE1, we found that icariin reduces secretion of sAPPβ which may have contributed to cognitive improvements observed in previous mouse model studies. Lastly, our screen identified progesterone as a Aβ-reducing compound. In previous in vivo studies, progesterone was shown to reduce amyloid load and improve cognitive performance of AD mouse models (Carroll et al., 2010; Frye and Walf, 2008). Since progesterone lowered sAPPβ, Aβ40 and Aβ42 production in neurons, it is conceivable that Aβ-reducing activity may underlie the observed rescue of pathological and behavioral changes in mouse models of AD. Collectively, our approach therefore could be useful in evaluating potential of known drugs for a new use in AD in the context of phenotypically intact neurons as well as screening for novel small molecules.

EXPERIMENTAL PROCEDURES

Directed differentiation of mouse embryonic stem cells to pyramidal neurons

mES were maintained for two passages on mouse embryonic fibroblast (MEF) feeder cells in the presence of Leukemia Inhibitory Factor (LIF) (Millipore). For embryoid body (EB) formation, mES were deprived of MEFs for two passages. EB were grown in suspension for 8 days and in the presence of retinoic acid (RA) for the last 4 days prior to plating as neurons. Optimized neuronal media containing N2 supplement (Invitrogen) was used for the

first 2 days after plating and B27 (Invitrogen) supplemented media was used for the duration of the culture. Detailed media composition and protocols are found in Supplemental Experimental Methods.

Analysis of synaptic proteins, morphology and spine density

After DIV21, ESN were treated with 200nM Aβ oligomer prepared as previously described (Dahlgren et al., 2002; McIntire et al., 2012) for 24 hours then fixed in 4% paraformaldehyde and 4% sucrose in PBS for 20 minutes. PSD-95 (Thermo Scientific) and synaptophysin (S-physin) (Epitomics) antibodies were used and detected with Alexa tagged secondary antibodies (Molecular Probes). For spine analysis, after fixation, neurons were labeled with DiI (Molecular Probes) as previously described (Moolman et al., 2004; McIntire et al., 2012). Images were collected with an inverted Olympus microscope with 100x objective using Nikon C2 confocal laser microscope system. For spine analysis, 0.5μM z-sections were taken at 3x zoom. Images were stacked, used for 2-D projection with ImageJ 1.4g software (NIH), and measured with the segmented line tool. For particle analysis, the RGB colors were split, threshold was set for each image, and the analyze particles tool was used.

Phospho-CREB detection

Neurons were grown to maturity and pre-treated for 1 hour in the presence or absence of Aβ oligomer preparation. Subsequently, cultures were treated 10 minutes under stimulating conditions (150mM, 5mM KCl, 2mM $CaCl_2$, 30mM glucose, 10mM HEPES, pH7.4, 10μM NMDA) (Synder et al., 2005) or non-stimulating conditions (120mM NaCl, 3mM KCl, 2mM $CaCl_2$, 2mM $MgCl_2$, 15mM glucose, 15mM HEPES, pH 7.4) in the presence or absence of Aβ oligomer (Dahlgren et al., 2002). Protein was solubilized immediately in Laemmli sample buffer and loaded (v/v) to 4-20% Tris/Glycine gel (Invitrogen). Protein was separated using SDS-PAGE and quantitative Western blotting was accomplished using infra-red secondary antibody (Rockland) detection with the Licor Odyssey Infrared Imager with solid-state diode laser at 685 nm and 785 nm. Total CREB primary antibody was from Santa Cruz Biotechnology and phospho-CREB (S133) primary antibody was from Invitogen.

Subcellular Fractionation

Differentiated mouse embryonic stem cells were homogenized using a ball-bearing homogenizer in homogenization buffer (0.25M sucrose, 10mM Tris, pH7.4, 2mM MgAC, and 0.5 mM EDTA, supplemented with protease inhibitors (Roche)). Homogenate was loaded onto a 0.25M – 2M sucrose step gradient and centrifuged for 2.5h at 39,000rpm at 4°C. Ten fractions were collected and analyzed by Western blotting. Primary antibodies used were: anti-sortilin (BD Biosciences), anti-BACE1 (Zhoa et al., 2007), anti-APP-CTmax (Landman et al., 2006; Okada et al., 2010), anti-syn6 (BD Biosciences), anti-EEA1 (Affinity BioReagents) and anti-Rab11 (BD Biosciences).

Lentiviral Expression of APP_{sw} in ESNs and generation of FAD mutant PS1 stable ES cell lines

To model human APP processing, neurons were infected with APP_{sw} lentivirus for 24 hours and 48 hours after initial infection, treated with BACE inhibitor IV (BSI) (Calbiochem) or γ-secretase inhibitor (GSI) (Calbiochem) for 24 hours. Uninfected neurons were treated with 0.1% saponin (Sap) as a positive control for loss of cell viability. To generate stable lines of mES cells expressing PS1 wild-type and FAD variants 3×10^6 ES cells were resuspended in Nucleofector solution (Amaxa Neucleofector, Lonza) and mixed with 20 μg plasmid carrying human wild-type or FAD mutant PS1 and neomycin resistance in the pcDNA3.1

vector. Cells were electroporated using program A-13 (Amaxa), resuspended, plated on feeder cells and subjected to G418 (250-500 μg/ml) selection 24 hours after electroporation.

Analysis of APP processing

At DIV 12-30, neurons were infected with lentivirus carrying the Swedish variant of human APP (pLenti6/hAPP_{sw}). After 24 hrs, cell medium was changed and 48 hours after infection, cells were treated with secretase inhibitors. Conditioned media was collected after 24 hrs and the levels of Aβ42 and Aβ40 were determined using sandwich ELISA (Invitrogen) according to the manufacturer's protocol. Total protein levels were determined by BCA protein assay (Pierce). Total Aβ was detected by immunoprecipitating conditioned medium with 6E10 (Covance) or 7N22 (Invitrogen) antibodies, running samples on NuPAGE gels and detected by quantitative Western blotting with 6E10 antibody. Full-length APP was detected by Western blot analysis using 6E10 (Covance) or polyclonal antibody against the C-terminus of APP (APP-CTmax) (Landman et al., 2006; Okada et al., 2010). For detection of of sAPPβ and sAPPα conditioned medium was harvested 24 hours after a media change.

Immunoprecipitation of sAPPβ was performed using sβsw antibody (Figure S2). Protein G plus/Protein A agarose suspension (Calbiochem) was used to precipitate the antibody-protein complex. The immunoprecipitate was subjected to SDS-PAGE followed by Western blot detection using 22C11 (Chemicon) or LN27 (Covance). sAPPα was immunoprecipitated with 6E10 and detected on Western blot with LN27. BACE inhibitor IV, compound E and TAPI-2 were from Calbiochem.

Isolation of ES cells from a mouse model of AD

Tg2576 mice were outbred strain of Swiss Webster × B6D2F1 which is a C57BL/6 × DBA/2 F1 cross harboring the APP transgene with the Swedish mutation under the control of the prion promoter (Hsiao et al., 1996) C57BL/6 females 23 days old were induced for superovulation with a standard protocol using intraperitoneal injection with pregnant mares serum gonadotropin (PMSG) on day 1 and human chorionic gonadotropin (hCG) on day 3. Immediately following the final injection, the female was mated with a male positive for the APP_{sw} transgene. After 3.5 days blastocysts were flushed from the uterus and cultured in 96-well feeder plate wells containing mitomycin C-treated MEF feeders in ES medium for six days without medium change. Inner cell mass (ICM) outgrowth was disaggregated with 0.05% trypsin into small clumps and plated in one well of 24-well feeder plates. ES colonies were apparent on day three after re-plating and ES cells were passaged upon confluence and maintained as above. DNA was isolated using the DNeasy and Tissue DNA isolation kit (Qiagen). ES lines harboring the transgene were identified using PCR based genotyping protocol with primers against the human APP_{sw} gene sequence (sense primer 1: CCGAGATCTCTGAAGTGAAGATGGATG and antisense primer 2: GTGGATACCCCCTCCCCCAGCCTAGACC).

Small molecule screen of clinical compound library for reduction of Aβ

ESNs were plated in 96 well black plates at a density of 1.5×10^5 cells/cm^2 (45,000 cells/well). After DIV 8, ESNs were treated with 10μM of each compound from a library of 446 clinically relevant compounds which have a history of use in human, the NIH clinical collection (NCC) (NIH) for 24 hours in B27 media. Each plate of ESNs was treated additionally with DMSO (negative control), and positive controls for Aβ reduction, BSI and GSI using 6 replicates. After 24 hours, conditioned media was harvested and frozen at -80°C until Aβ40 analysis using human specific ELISA (Invitrogen). The remaining cells were subjected to cell viability assay CellQuanti Blue (BioAssay Systems). Compounds were considered hits if they reduced Aβ40 by 40% compared to the negative control (DMSO) and reduced Aβ40 by 4 standard deviations from the average value of the negative control but

maintained cell viability. Cell viability was defined by maintenance of CellQuanti Blue (BioAssay Systems) fluorescent signal within two standard deviations of the control treated (DMSO) neurons. For confirmation studies, amiridine, phenelzine and icariin were obtained from Sigma and progesterone was obtained from Tocris.

Supplementary Material

Refer to Web version on PubMed Central for supplementary material.

Acknowledgments

This work has been supported by Alzheimer's Association, NIH grants MN015174, and AG08702 to L.B.J.M. and NIH grant NS074536 and Alzheimer's Drug Discovery Foundation to T.W.K. This publication was supported by the National Center for Advancing Translational Sciences, National Institutes of Health, through Grant Number UL1 TR000040, formerly the National Center for Research Resources, Grant Number UL1 RR024156. The content is solely the responsibility of the authors and does not necessarily represent the official views of the NIH. We would like to thank K. Duff for the gift of the Tg2576 mice. The BACE1 antibody was a gift from R. Vassar and PS1 antibodies were kindly provided by J. Lah. We thank Jole Fiorito for help with the chemical structure images.

References

Abbott A. Neurologists strike gold in drug screen effort. Nature. 2002; 417:109. [PubMed: 12000928]

Barker RA. Stem cells and neurodegenerative diseases: where is it all going? Regen Med. 2012; 7:26–31. [PubMed: 23210808]

Bibel M, Richter J, Schrenk K, Tucker KL, Staiger V, Korte M, Goetz M, Barde YA. Differentiation of mouse embryonic stem cells into a defined neuronal lineage. Nat Neurosci. 2004; 7:1003–1009. [PubMed: 15332090]

Bibel M, Richter J, Lacroix E, Barde YA. Generation of a defined and uniform population of CNS progenitors and neurons from mouse embryonic stem cells. Nat Protoc. 2007; 2:1034–1043. [PubMed: 17546008]

Braginskaya FI, Zorina M, Pal'mina NP, Gaintseva VD, Burlakova EB, Selezneva ND, Kolykhalov IV, Gavrilova SI. Some blood biochemistry parameters during the cholinergic treatment of Alzheimer's disease. Neurosci Behav Physiol. 2001; 31:457–461. [PubMed: 11508499]

Buck CR, Martinez H, Chao MV, Black IB. Differential expression of the nerve growth factor receptor gene in multiple brain areas. Dev Brain Res. 1988; 44:259–268. [PubMed: 2852071]

Calabrese B, Shaked GM, Tabarean IV, Braga J, Koo EH, Halpain S. Rapid, concurrent alterations in pre- and postsynaptic structure induced by naturally-secreted amyloid-beta protein. Mol Cell Neurosci. 2007; 35:183–93. [PubMed: 17368908]

Carroll JC, Rosario ER, Chang L, Stanczyk FZ, Oddo S, LaFerla FM, Pike CJ. Progesterone and estrogen regulate Alzheimer-like neuropathology in female 3xTg-AD mice. J Neurosci. 2007; 27:13357–13365. [PubMed: 18045930]

Carroll JC, Rosario ER, Chang L, Stanczyk FZ, Oddo S, LaFerla FM, Pike CJ. Progesterone and estrogen regulate Alzheimer-like neuropathology in female 3xTg-AD mice. J Neurosci. 2007; 27:13357–13365. [PubMed: 18045930]

Carroll JC, Rosario ER, Villamagna A, Pike CJ. Continuous and cyclic progesterone differentially interact with estradiol in the regulation of Alzheimer-like pathology in female 3xTransgenic-Alzheimer's disease mice. Endocrinology. 2010; 151:2713–2722. [PubMed: 20410196]

Cerpa W, Farías GG, Godoy JA, Fuenzalida M, Bonansco C, Inestrosa NC. Wnt-5a occludes Abeta oligomer-induced depression of glutamatergic transmission in hippocampal neurons. Mol Neurodegener. 2010; 5:3. [PubMed: 20205789]

Chan CH, Godinho LN, Thomaidou D, Tan SS, Gulisano M, Parnavelas JG. Emx1 is a marker for pyramidal neurons of the cerebral cortex. Cereb Cortex. 2001; 11:1191–1198. [PubMed: 11709490]

Choi SH, Tanzi RE. iPSCs to the rescue in Alzheimer's research. Cell Stem Cell. 2012; 10:235–236. [PubMed: 22385650]

Dahlgren KN, Manelli AM, Stine WB Jr, Baker LK, Krafft GA, LaDu MJ. Oligomeric and fibrillar species of amyloid-beta peptides differentially affect neuronal viability. J Biol Chem. 2002; 277:32046–32053. [PubMed: 12058030]

Dhara SK, Stice SL. Neural differentiation of human embryonic stem cells. J Cell Biochem. 2008; 105:633–640. [PubMed: 18759328]

Ebert AD, Svendsen CN. Human stem cells and drug screening: opportunities and challenges. Nat Rev Drug Discov. 2010; 9:367–372. [PubMed: 20339370]

Engle SJ, Puppala D. Integrating Human Pluripotent Stem Cells into Drug Development. Cell Stem Cell. 2013; 12:669. [PubMed: 23746976]

Erceg S, Ronaghi M, Stojković M. Human embryonic stem cell differentiation toward regional specific neural precursors. Stem Cells. 2009; 27:78–87. [PubMed: 18845761]

Finan GM, Okada H, Kim T-W. BACE1 Retrograde Trafficking is Uniquely Regulated by the Cytoplasmic Domain of Sortilin. J Biol Chem. 2011; 286:12602–12616. [PubMed: 21245145]

Freedman M, Rewilak D, Xerri T, Cohen S, Gordon AS, Shandling M, Logan AG. L-deprenyl in Alzheimer's disease: cognitive and behavioral effects. Neurology. 1998; 50:660–668. [PubMed: 9521253]

Frye CA, Walf AA. Effects of progesterone administration and APP_{swe}+PSEN1Deltae9 mutation for cognitive performance of mid-aged mice. Neurobiol Learn Mem. 2008; 89:17–26. [PubMed: 17988898]

Gylys KH, Fein JA, Yang F, Wiley DJ, Miller CA, Cole GM. Synaptic changes in Alzheimer's disease: increased amyloid-beta and gliosis in surviving terminals is accompanied by decreased PSD-95 fluorescence. J Pathol. 2004; 165:1809–17.

Han SS, Williams LA, Eggan KC. Constructing and deconstructing stem cell models of neurological disease. Neuron. 2011; 70:626–644. [PubMed: 21609821]

Hardy J, Selkoe DJ. The amyloid hypothesis of Alzheimer's disease: progress and problems on the road to therapeutics. Science. 2002; 297:353–356. [PubMed: 12130773]

Hsiao K, Chapman P, Nilsen S, Eckman C, Harigaya Y, Younkin S, Yang F, Cole G. Correlative memory deficits, Abeta elevation, and amyloid plaques in transgenic mice. Science. 1996; 274:99–102. [PubMed: 8810256]

Hsieh H, Boehm J, Sato C, Iwatsubo T, Tomita T, Sisodia S, Malinow R. AMPAR removal underlies Abeta-induced synaptic depression and dendritic spine loss. Neuron. 2006; 52:831–843. [PubMed: 17145504]

Hu L, Wong TP, Côté SL, Bell KF, Cuello AC. The impact of Abeta-plaques on cortical cholinergic and non-cholinergic presynaptic boutons in alzheimer's disease-like transgenic mice. Neuroscience. 2003; 121:421–432. [PubMed: 14522000]

Inglese J, Johnson RL, Simeonov A, Xia M, Zheng W, Austin CP, Auld DS. High-throughput screening assays for the identification of chemical probes. Nat Chem Biol. 2007; 3:466–479. [PubMed: 17637779]

Israel MA, Yuan SH, Bardy C, Reyna SM, Mu Y, Herrera C, Hefferan MP, Van Gorp S, Nazor KL, Boscolo FS, Carson CT, Laurent LC, Marsala M, Gage FH, Remes AM, Koo EH, Goldstein LS. Probing sporadic and familial Alzheimer's disease using induced pluripotent stem cells. Nature. 2012; 482:216–220. [PubMed: 22278060]

Jacobsen JS, Wu CC, Redwine JM, Comery TA, Arias R, Bowlby M, Martone R, Morrison JH, Pangalos MN, Reinhart PH, Bloom FE. Early-onset behavioral and synaptic deficits in a mouse model of Alzheimer's disease. Proc Natl Acad Sci U S A. 2006; 103:5161–5166. [PubMed: 16549764]

Jang J, Yoo JE, Lee JA, Lee DR, Kim JY, Huh YJ, Kim DS, Park CY, Hwang DY, Kim HS, Kang HC, Kim DW. Disease-specific induced pluripotent stem cells: a platform for human disease modeling and drug discovery. Exp Mol Med. 2012; 44:202–213. [PubMed: 22179105]

Kim JE, O'Sullivan ML, Sanchez CA, Hwang M, Israel MA, Brennand K, Deerinck TJ, Goldstein LS, Gage FH, Ellisman MH, Ghosh A. Investigating synapse formation and function using human pluripotent stem cell-derived neurons. Proc Natl Acad Sci U S A. 2011; 108:3005–3010. [PubMed: 21278334]

King DL, Arendash GW. Maintained synaptophysin immunoreactivity in Tg2576 transgenic mice during aging: correlations with cognitive impairment. Brain Res. 2002; 926:58–68. [PubMed: 11814407]

Lacor PN, Buniel MC, Furlow PW, Clemente AS, Velasco PT, Wood M, Viola KL, Klein WL. Abeta oligomer-induced aberrations in synapse composition, shape, and density provide a molecular basis for loss of connectivity in Alzheimer's disease. J Neurosci. 2007; 27:796–807. [PubMed: 17251419]

Landman N, Jeong SY, Shin SY, Voronov SV, Serban G, Kang MS, Park MK, Di Paolo G, Chung S, Kim TW. Presenilin mutations linked to familial Alzheimer's disease cause an imbalance in phosphatidylinositol 4,5-bisphosphate metabolism. Proc Natl Acad Sci U S A. 2006; 103:19524–19529. [PubMed: 17158800]

Lee JH, Ko E, Kim YE, Min JY, Liu J, Kim Y, Shin M, Hong M, Bae H. Gene expression profile analysis of genes in rat hippocampus from antidepressant treated rats using DNA microarray. BMC Neurosci. 2010; 11:152. [PubMed: 21118505]

Li L, Tsai HJ, Li L, Wang XM. Icariin inhibits the increased inward calcium currents induced by amyloid-beta(25-35) peptide in CA1 pyramidal neurons of neonatal rat hippocampal slice. Am J Chin Med. 2010; 38:113–125. [PubMed: 20128049]

Lichtenthaler SF, Dominguez DI, Westmeyer GG, Reiss K, Haass C, Saftig P, De Strooper B, Seed B. The cell adhesion protein P-selectin glycoprotein ligand-1 is a substrate for the aspartyl protease BACE1. J Biol Chem. 2003; 278:48713–48719. [PubMed: 14507929]

Mangialasche F, Solomon A, Winblad B, Mecocci P, Kivipelto M. Alzheimer's disease: clinical trials and drug development. Lancet Neurol. 2010; 9:702–716. [PubMed: 20610346]

Mangoni A, Grassi MP, Frattola L, Piolti R, Bassi S, Motta A, Marcone A, Smirne S. Effects of a MAO-B inhibitor in the treatment of Alzheimer disease. Eur Neurol. 1991; 31:100–107. [PubMed: 1904354]

Mann DM. Pyramidal nerve cell loss in Alzheimer's disease. Neurodegeneration. 1996; 5:423–7. [PubMed: 9117557]

McIntire LB, Berman DE, Myaeng J, Staniszewski A, Arancio O, Di Paolo G, Kim TW. Reduction of synaptojanin 1 ameliorates synaptic and behavioral impairments in a mouse model of Alzheimer's disease. J Neurosci. 2012; 32:15271–15276. [PubMed: 23115165]

McNeish J. Embryonic stem cells in drug discovery. Nat Rev Drug Discov. 2004; 3:70–80. [PubMed: 14708022]

Moolman DL, Vitolo OV, Vonsattel JP, Shelanski ML. Dendrite and dendritic spine alterations in Alzheimer models. J Neurocytol. 2004; 33:377–387. [PubMed: 15475691]

Morrison JH, Hof PR. Selective vulnerability of corticocortical and hippocampal circuits in aging and Alzheimer's disease. Prog Brain Res. 2002; 136:467–86. [PubMed: 12143403]

Nie J, Luo Y, Huang XN, Gong QH, Wu Q, Shi JS. Icariin inhibits beta-amyloid peptide segment 25-35 induced expression of beta-secretase in rat hippocampus. Eur J Pharmacol. 2010; 626:213–218. [PubMed: 19782061]

Nistor G, Siegenthaler MM, Poirier SN, Rossi S, Poole AJ, Charlton ME, McNeish JD, Airriess CN, Keirstead HS. Derivation of high purity neuronal progenitors from human embryonic stem cells. PLoS One. 2011; 6:e20692. [PubMed: 21673956]

Noorbakhsh F, Overall CM, Power C. Deciphering complex mechanisms in neurodegenerative diseases: the advent of systems biology. Trends Neurosci. 2009; 32:88–100. [PubMed: 19135729]

O'Brien RJ, Wong PC. Amyloid Precursor Protein Processing and Alzheimer's Disease. Annu Rev Neurosci. 2011; 34:185–204. [PubMed: 21456963]

Ogura H, Kosasa T, Kuriya Y, Yamanishi Y. Comparison of inhibitory activities of donepezil and other cholinesterase inhibitors on acetylcholinesterase and butyrylcholinesterase in vitro. Methods Find Exp Clin Pharmacol. 2000; 22:609–613. [PubMed: 11256231]

Okada H, Zhang W, Peterhoff C, Hwang JC, Nixon RA, Ryu SH, Kim TW. Proteomic identification of sorting nexin 6 as a negative regulator of BACE1-mediated APP processing. FASEB J. 2010; 24:2783–2794. [PubMed: 20354142]

Ooi L, Sidhu K, Poljak A, Sutherland G, O'Connor MD, Sachdev P, Münch G. Induced pluripotent stem cells as tools for disease modeling and drug discovery in Alzheimer's disease. J Neural Transm. 2013; 120:103–111. [PubMed: 22695755]

Papp B, Plath K. Reprogramming to pluripotency: stepwise resetting of the epigenetic landscape. Cell Res. 2011; 21:486–501. [PubMed: 21321600]

Pouton CW, Haynes JM. Embryonic stem cells as a source of models for drug discovery. Nat Rev Drug Discov. 2007; 6:605–616. [PubMed: 17667955]

Pozueta J, Lefort R, Shelanski ML. Synaptic changes in Alzheimer's disease and its models. Neuroscience. 2012 in press.

Roselli F, Tirard M, Lu J, Hutzler P, Lamberti P, Livrea P, Morabito M, Almeida OF. Soluble beta-amyloid1-40 induces NMDA-dependent degradation of postsynaptic density-95 at glutamatergic synapses. J Neurosci. 2005; 25:11061–11070. [PubMed: 16319306]

Rubin LL, Haston KM. Stem cell biology and drug discovery. BMC Biol. 2011; 9:42. [PubMed: 21649940]

Schwartz PH, Brick DJ, Stover AE, Loring JF, Müller FJ. Differentiation of neural lineage cells from human pluripotent stem cells. Methods. 2008; 45:142–158. [PubMed: 18593611]

Seiffert D, Bradley JD, Rominger CM, Rominger DH, Yang F, Meredith JE Jr, Wang Q, Roach AH, Thompson LA, Spitz SM, Higaki JN, Prakash SR, Combs AP, Copeland RA, Arneric SP, Hartig PR, Robertson DW, Cordell B, Stern AM, Olson RE, Zaczek R. Presenilin-1 and -2 are molecular targets for gamma-secretase inhibitors. J Biol Chem. 2000; 275:34086–34091. [PubMed: 10915801]

Sano M, Ernesto C, Thomas RG, Klauber MR, Schafer K, Grundman M, Woodbury P, Growdon J, Cotman CW, Pfeiffer E, Schneider LS, Thal LJ. A controlled trial of selegiline, alpha-tocopherol, or both as treatment for Alzheimer's disease. The Alzheimer's Disease Cooperative Study. N Engl J Med. 1997; 336:1216–1222. [PubMed: 9110909]

Shankar GM, Bloodgood BL, Townsend M, Walsh DM, Selkoe DJ, Sabatini BL. Natural oligomers of the Alzheimer amyloid-beta protein induce reversible synapse loss by modulating an NMDA-type glutamate receptor-dependent signaling pathway. J Neurosci. 2007; 27:2866–2875. [PubMed: 17360908]

Snyder EM, Nong Y, Almeida CG, Paul S, Moran T, Choi EY, Nairn AC, Salter MW, Lombroso PJ, Gouras GK, Greengard P. Regulation of NMDA receptor trafficking by amyloid-beta. Nat Neurosci. 2005; 8:1051–1058. [PubMed: 16025111]

Stachel SJ, Coburn CA, Steele TG, Crouthamel MC, Pietrak BL, Lai MT, Holloway MK, Munshi SK, Graham SL, Vacca JP. Conformationally biased P3 amide replacements of beta-secretase inhibitors. Bioorg Med Chem Lett. 2006; 16:641–644. [PubMed: 16263281]

Tang BL. Neuronal protein trafficking associated with Alzheimer disease: from APP and BACE1 to glutamate receptors. Cell Adh Migr. 2009; 3:118–128. [PubMed: 19372755]

Urano T, Tohda C. Icariin improves memory impairment in Alzheimer's disease model mice (5xFAD) and attenuates amyloid β-induced neurite atrophy. Phytother Res. 2010; 24:1658–1663. [PubMed: 21031624]

Vitolo OV, Sant'Angelo A, Costanzo V, Battaglia F, Arancio O, Shelanski M. Amyloid beta -peptide inhibition of the PKA/CREB pathway and long-term potentiation: reversibility by drugs that enhance cAMP signaling. Proc Natl Acad Sci USA. 2002; 99:13217–13221. [PubMed: 12244210]

Volz HP, Gleiter CH. Monoamine oxidase inhibitors. A perspective on their use in the elderly. Drugs Aging. 1998; 13:341–355. [PubMed: 9829163]

Weinreb O, Mandel S, Bar-Am O, Yogev-Falach M, Avramovich-Tirosh Y, Amit T, Youdim MB. Multifunctional neuroprotective derivatives of rasagiline as anti-Alzheimer's disease drugs. Neurotherapeutics. 2009; 6:163–174. [PubMed: 19110207]

Wen L, Tang FL, Hong Y, Luo SW, Wang CL, He W, Shen C, Jung JU, Xiong F, Lee DH, Zhang QG, Brann D, Kim TW, Yan R, Mei L, Xiong WC. VPS35 haploinsufficiency increases Alzheimer's disease neuropathology. J Cell Biol. 2011; 195:765–779. [PubMed: 22105352]

Wong PC, Zheng H, Chen H, Becher MW, Sirinathsinghji DJ, Trumbauer ME, Chen HY, Price DL, Van der Ploeg LH, Sisodia SS. Presenillin 1 is required for notch-1 and DII1expression in the paraxial mesoderm. Nature. 1997; 387:288–292. [PubMed: 9153393]

Yagi T, Ito D, Okada Y, Akamatsu W, Nihei Y, Yoshizaki T, Yamanaka S, Okano H, Suzuki N. Modeling familial Alzheimer's disease with induced pluripotent stem cells. Hum Mol Genet. 2011; 20:4530–4539. [PubMed: 21900357]

Yamanaka S, Blau HM. Nuclear reprogramming to a pluripotent state by three approaches. Nature. 2010; 465:704–712. [PubMed: 20535199]

Yoshida S, Suzuki N. Antiamnesic and cholinomimetic side-effects of the cholinesterase inhibitors, physostigmine, tacrine and NIK-247 in rats. Eur J Pharmacol. 1993; 250:117–124. [PubMed: 8119309]

Youdim MB, Amit T, Bar-Am O, Weinstock M, Yogev-Falach M. Amyloid processing and signal transduction properties of antiparkinson-antialzheimer neuroprotective drugs rasagiline and TV3326. Ann N Y Acad Sci. 2003; 993:378–386. [PubMed: 12853332]

Zeng KW, Ko H, Yang HO, Wang XM. Icariin attenuates β-amyloid-induced neurotoxicity by inhibition of tau protein hyperphosphorylation in PC12 cells. Neuropharmacology. 2010; 59:542–550. [PubMed: 20708632]

Zhao J, Fu Y, Yasvoina M, Shao P, Hitt B, O'Connor T, Logan S, Maus E, Citron M, Berry R, Binder L, Vassar R. Beta-site amyloid precursor protein cleaving enzyme 1 levels become elevated in neurons around amyloid plaques: implications for Alzheimer's disease pathogenesis. J Neurosci. 2007; 27:3639–3649. [PubMed: 17409228]

Zheng H, Koo EH. Biology and Pathophysiology of the Amyloid Precursor Protein. Mol Neurodegener. 2011; 6:27. [PubMed: 21527012]

HIGHLIGHTS

- Scaling and optimizing primary neurons derived from mouse ES cells
- Modeling phenotypic assays using mouse ESNs for biogenesis and synaptic action of Aβ
- Isolation and use of ES cells originating from a mouse model of AD
- Screen of clinical compounds and identification of Aβ-lowering small molecules

SIGNIFICANCE

Our current study describes practical applications of mouse embryonic stem (ES) cell-derived neurons (ESNs) for AD and CNS drug discovery research. Our studies indicate that ESNs could potentially replace dissociated primary neuron cultures as a cell-based model for investigation of neurobiology and pathobiology relevant to AD. We also demonstrated that ESNs from the Tg2576 mouse model of AD can be cultured and assayed in a platform suitable for drug screening. Using this ESN-based assay, we performed phenotypic screening assays and identified four interesting clinical compounds for which Aβ-modulating effects have not been previously reported in primary neurons. There is a growing demand for preclinical models that reliably predict efficacy and safety prior to clinical trials. This demand can be met by specialized disease-relevant cell types. For drug discovery applications, our system offers notable advantages over human patient derived stem cells, which have limited expandability and phenotypic variability. Thus, our model overcomes current challenges in phenotypic HTS assays in neurons, bridging the gap between in vitro screening paradigms and translational drug discovery and has great potential to lead to innovation in AD drug discovery by furnishing pyramidal neurons amenable to screening and functional evaluation of compound efficacy and toxicity in stem cell-derived primary neurons.

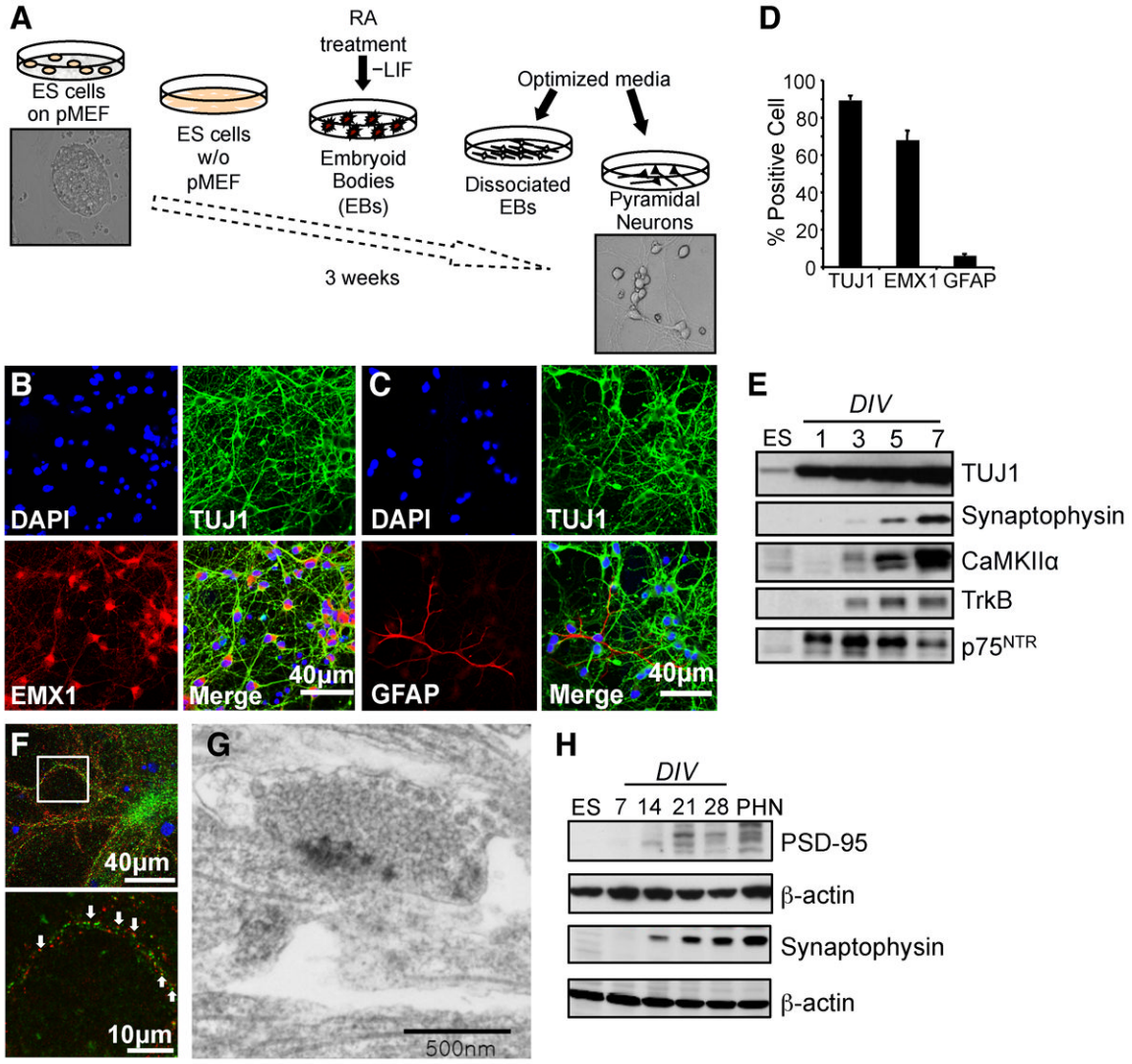

Figure 1. Directed Differentiation of mES Cells Into Pyramidal Cell-enriched Neurons

(A) Schematic of the differentiation procedure for mES cell derived neurons using primary mouse embryonic fibroblasts (pMEF) and retinoic acid (RA) showing ES cells and ESNs at DIV 5. (B) ES cell derived neuronal culture at DIV 7 co-labeled with neuronal β-tubulin III (TUJ1) and EMX1 antibodies and DAPI to identify nuclei. (C) ES cell derived neuronal culture at DIV 7 co-stained with GFAP antibody and TUJ1 antibodies and DAPI to identify nuclei. (D) Quantification of cultures show only 6(±1.5) % of cells stained positive for GFAP, while 68(±10)% cells were positive for EMX1 and 89.5 (±4)% cells were positive for TUJ1. Scale bar represents 40μm. (E) Cultures increasingly express neuronal proteins assessed by Western analysis using indicated antibodies. (F) Confocal images of *DIV21* neurons derived from mES cells detect post-synaptic density protein PSD-95 and pre-synaptic density protein synaptophysin which localize to adjacent puncta at higher magnification. (G) Electron micrograph showing intact synaptic structures including post-synaptic density and pre-synaptic vesicles in *DIV* 21 cultures. (H) PSD-95 and synaptophysin (S-physin) detection by Western analysis.

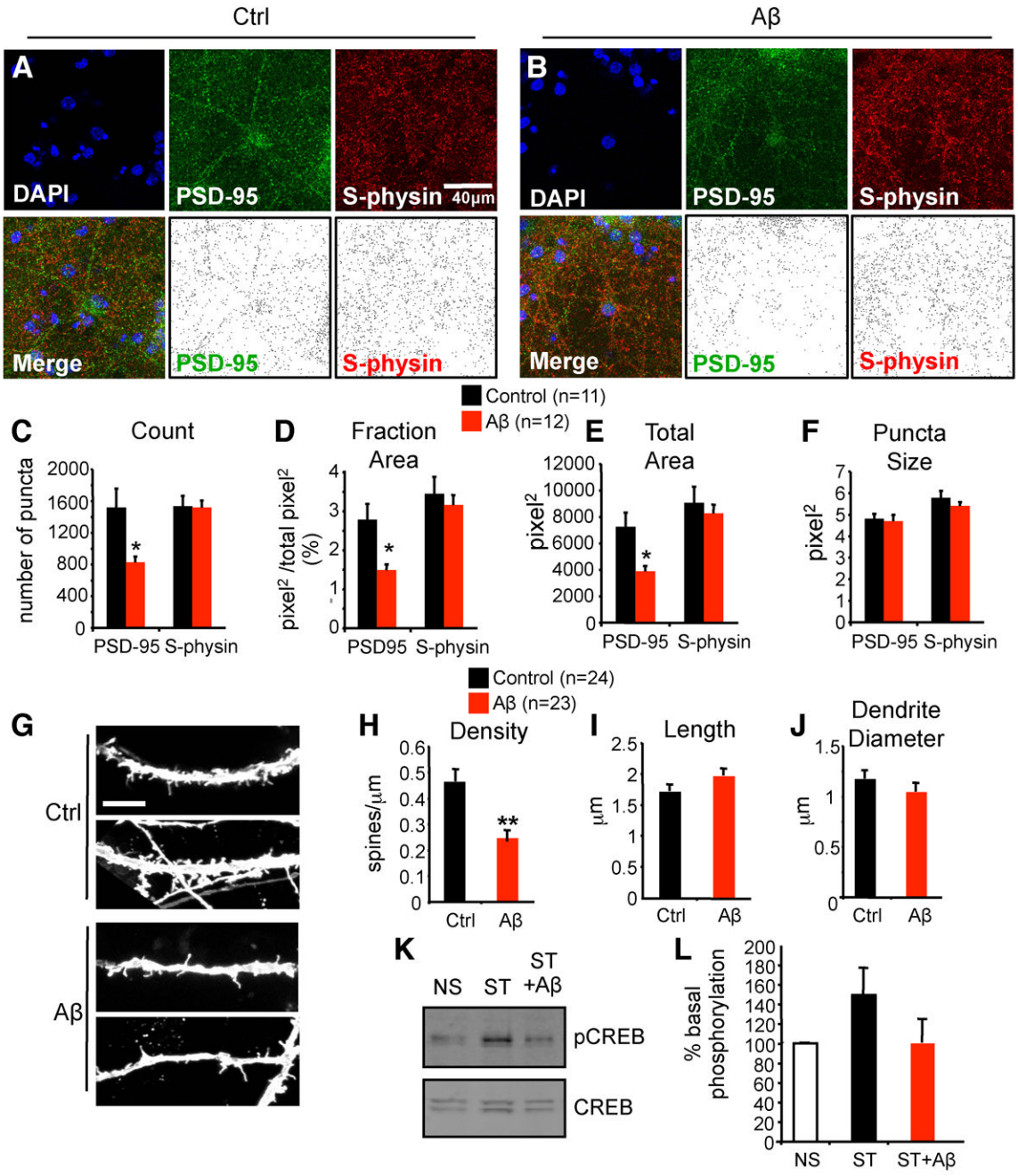

Figure 2. Modeling Aβ-associated Synaptic Abnormalities in ESNs

(A and B) At DIV 21 mES derived neurons were treated for 24 hours with DMSO control (Ctrl) or Aβ42 oligomer, subsequently fixed and co-stained for synaptic proteins PSD-95 (green) and synpatophysin (S-physin) (red). Nuclei are labeled with DAPI (blue). PSD-95 and S-physin particles were analyzed using Image J software. (C-F) Quantification of PSD-95 positive particles and S-physin positive particles using Image J software particle analysis. (G) DIV 21 ESN were treated with control or Aβ42 oligomer, fixed, diolistically labeled and imaged with confocal microscopy. (H-J) Spine density, length and dendrite diameter were quantified using Image J software. (K) Phosphorylation of CREB was detected with a pCREB specific antibody after no stimulation (NS) or NMDA stimulation

(ST) of cultures with or without Aβ42 oligomer (Aβ) pretreatment. (L) Quantification of CREB and pCREB using infrared quantitative Western blot imaging system with SEM shown by error bars.

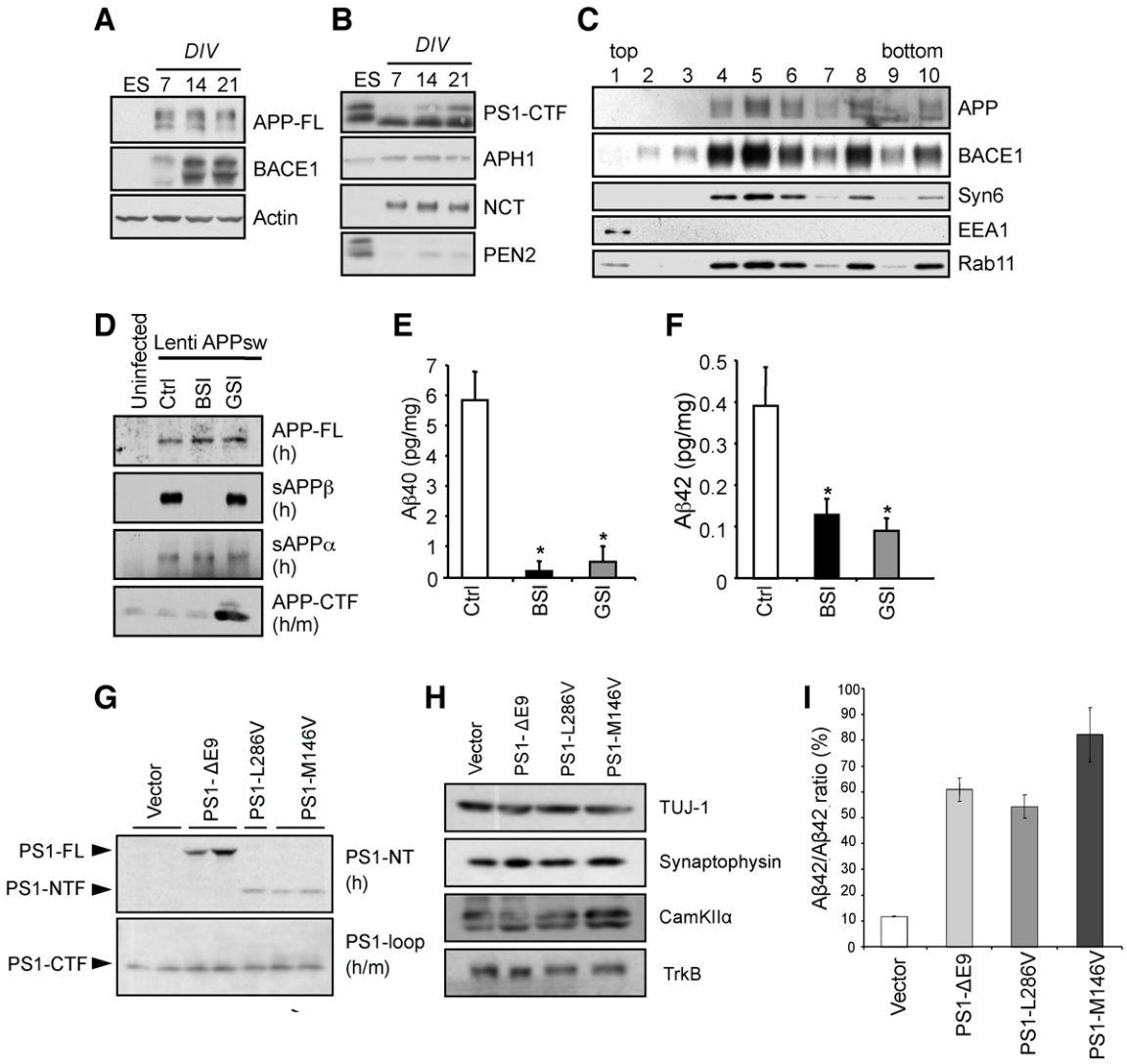

Figure 3. ESNs Harbor Machinery for APP Processing and Recapitulate Phenotype Associated with PS1 FAD

(A) APP and BACE1 expression in mES cells and ESNs at DIV 7, 14 and 21. (B) Components of the γ-secretatse, PS1, APH-1, NCT and PEN2 detected by Western blot analysis of the cell lysates using indicated antibodies. (C) Gradient centrifugation shows APP and BACE1 are enriched in the late endosome compartment with Syn6 and Rab11 but not at the top of the gradient with EEA1. (D) Western blot analysis of protein lysates from mES cell derived neurons infected with Lentivirus harboring human APP_{sw} expressing APP and proteolytic fragents. Secreted APP fragments, sAPPβ and sAPPα, were immunoprecipitated from conditioned media and APP and CTFs were detected in cell lysates. (E-F) Aβ40 and Aβ42 were detected in conditioned medium using human specific ELISA and values were normalized to protein lysate concentration. (G) Three different FAD mutants of PS1 (ΔE9, M146V, and L286V) were introduced into mES cells which were subsequently subjected to directed differentiation into pyramidal neurons. A representative Western blot shows transgene expression in the neurons derived from these clonal mES cell lines using an anti-human PS1 specific antibody (PS1-NT). (H) PS FAD-expressing cells undergo normal directed differentiation into pyramidal neurons indicated by expression of neuronal proteins. (I) ELISA detection of Aβ42 and Aβ40 from conditioned media of ESNs

stably expressing PS-FAD mutants infected at DIV 7 or 14 with APP_{sw} Lentiviral particles resulted in enhanced ratio of Aβ42/Aβ40. Lentiviral gene transfer did not affect the viability of ESNs (data not shown).

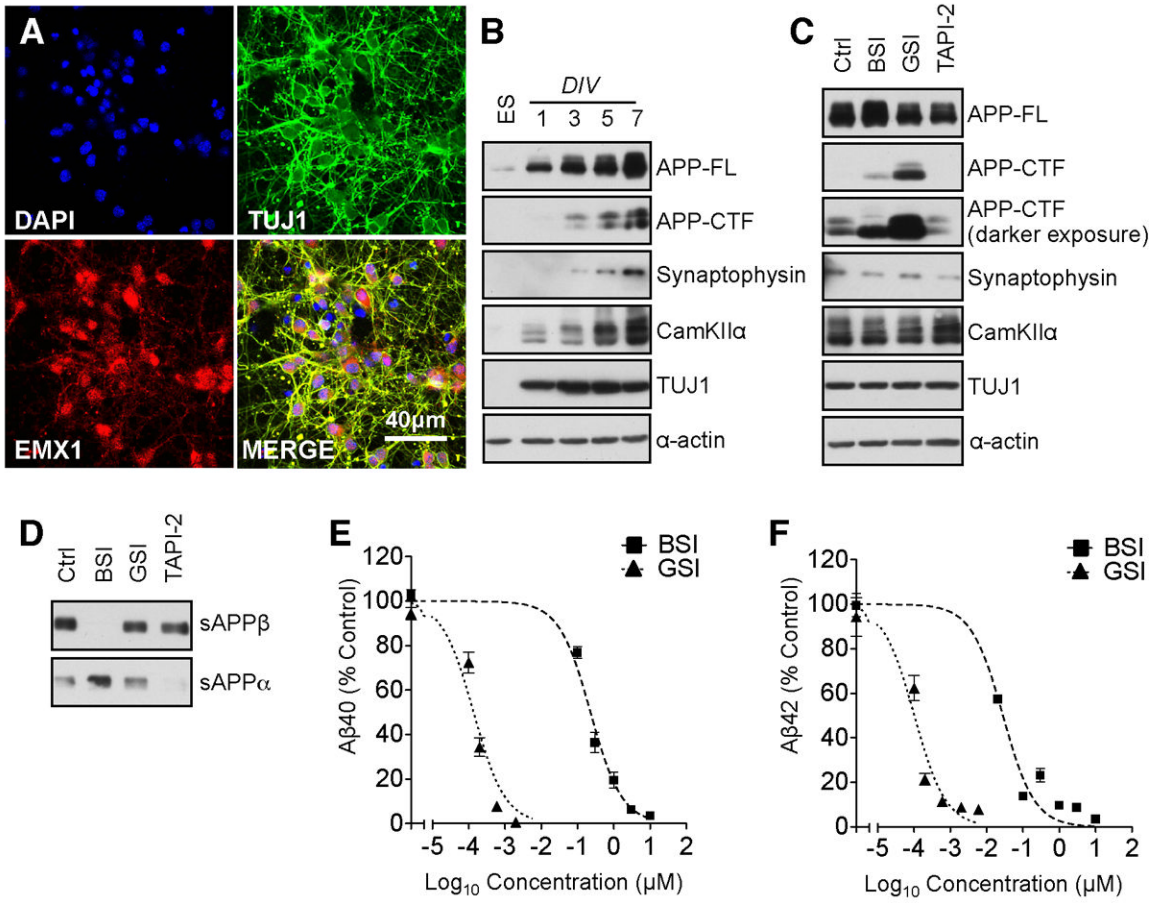

Figure 4. Analysis of mES Cells and ESNs Isolated From Tg2576 AD Mouse Model

(A) Tg2576 mES-derived neurons identified by nuclear DAPI stain, express neuronal β-tubulinIII (TUJ-1) (green) and pyramidal cell protein EMX1 (red). Scale bar represents 40μm. (B) Western blot analysis of protein lysates from Tg2576 mES-derived neuronal culture harvested at indicated *DIV* express APP, cleaved APP fragments (APP-CTF) and neuronal proteins synaptophysin, CamKIIα and neuronal β-tubulinIII (TUJ-1). α-Actin is a loading control. (C) Cell lysates from *DIV* 7 Tg2576 ES-derived neurons treated with indicated compounds were subjected to Western blot detection with 6E10 (APP-FL), APP-CTmax (APP-CTF) and antibodies to indicated proteins. (D) Secreted sAPPα and APPβ were immunoprecipitated from conditioned medium after treatment of Tg2576 ES-derived neurons with the indicated compounds. (E, F) Secreted Aβ levels detected using human specific Aβ40 or 42 ELISA kit. Aβ40 and Aβ42 show characteristic sensitivity to BSI and GSI inhibition. IC_{50} values for the BACE1 inhibitor were 229.7nM and 28.1nM for Aβ40 and Aβ42 respectively. IC_{50} values for Compound E were 136.9pM and 102.2pM Aβ40 and Aβ42 respectively. The Z' factors were 0.85 for Aβ40 and 0.5 for Aβ42 indicating an excellent assay for HTS.

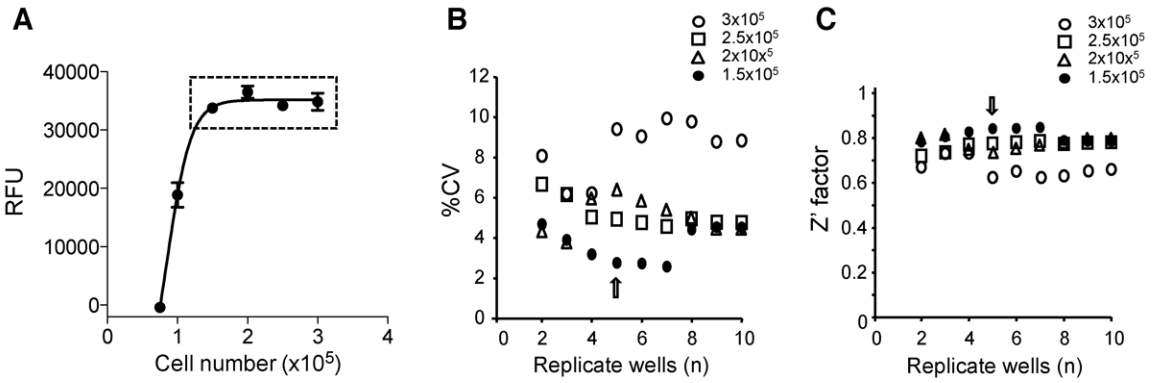

Figure 5. Miniaturization and Optimization of 96 Well Platform for Mouse ESNs

(A) DIV 8 Tg2576 ES-derived neurons were plated at increasing density in a 96 well plate and subjected to a cell viability assay quantified in relative fluorescent units (RFU). (B) %CV and (C) Z' were calculated with increasing number of wells. The minimum %CV and maximum Z' are optimized at n=5 wells at a plating density of 1.5×10^5 cells/cm^2 (arrows in B and C).

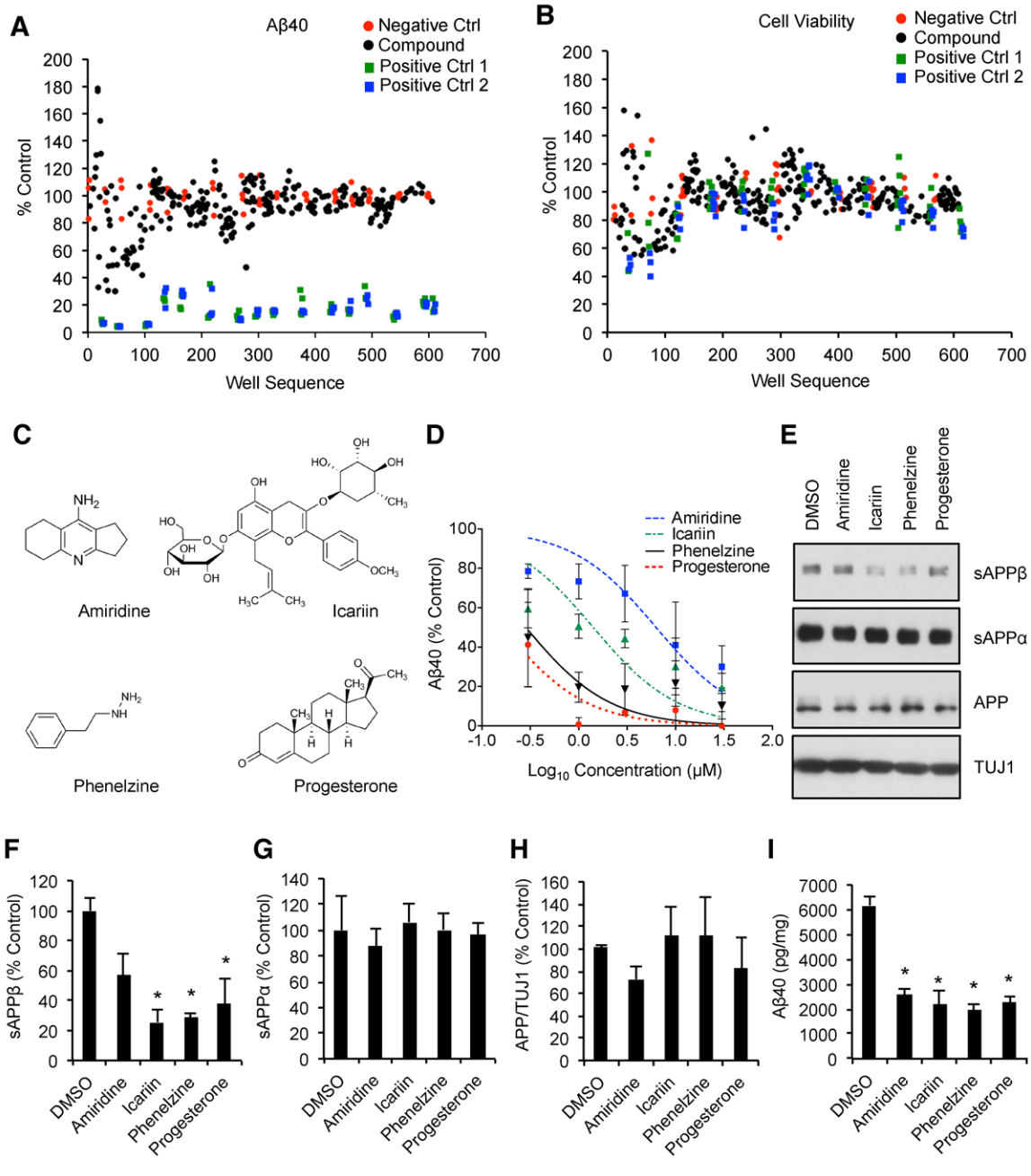

Figure 6. Screening NIH Clinical Collection (NCC) for Aβ Biogenesis

(A) DIV 7 Tg2576 ESNs plated in 96 well plate platform were treated with compounds from the NCC compound collection for 24 hours and Aβ40 was detected in conditioned media and is shown as % Control, DMSO treated wells. Negative control (Ctrl) was DMSO, while Positive Ctrl 1 was BACE inhibitor IV and Positive Ctrl 2 was Compound E. (B) The remaining cells were subjected to cell viability assay CellQuanti Blue. (C) Potent hits were obtained from an independent source and subjected to IC50 determination in the 96-well platform for Aβ40 biogenesis (Amiridine, 6.29 μM; Icariin, 1.412 μM; Phenelzine, 0.2834 μM; Progesterone, 0.1746 μM) determined by Prism analysis log(inhibitor) vs. normalized response curve fit with baseline level of Aβ40 subtracted. (D) Chemical structures of hit compounds(E) Representative Western blot analysis of APP processing determined using

immunoprecipitation of secreted fragments α and β from condition media. Full length APP was determined in protein lysate using Western blot analysis with 6E10 antibody and CTFs were detected using CTMaxi antibody. Neuronal β-tubulin was detected using TUJ1. (F,G) Quantification of sAPPβ and sAPPα (H) Full length APP was quantified by Image J analysis and normalized to tubulin (TUJ1). (I) Quantification of Aβ40 after treatment with indicated compounds normalized to protein level. Shown are means and SEM (n=3).

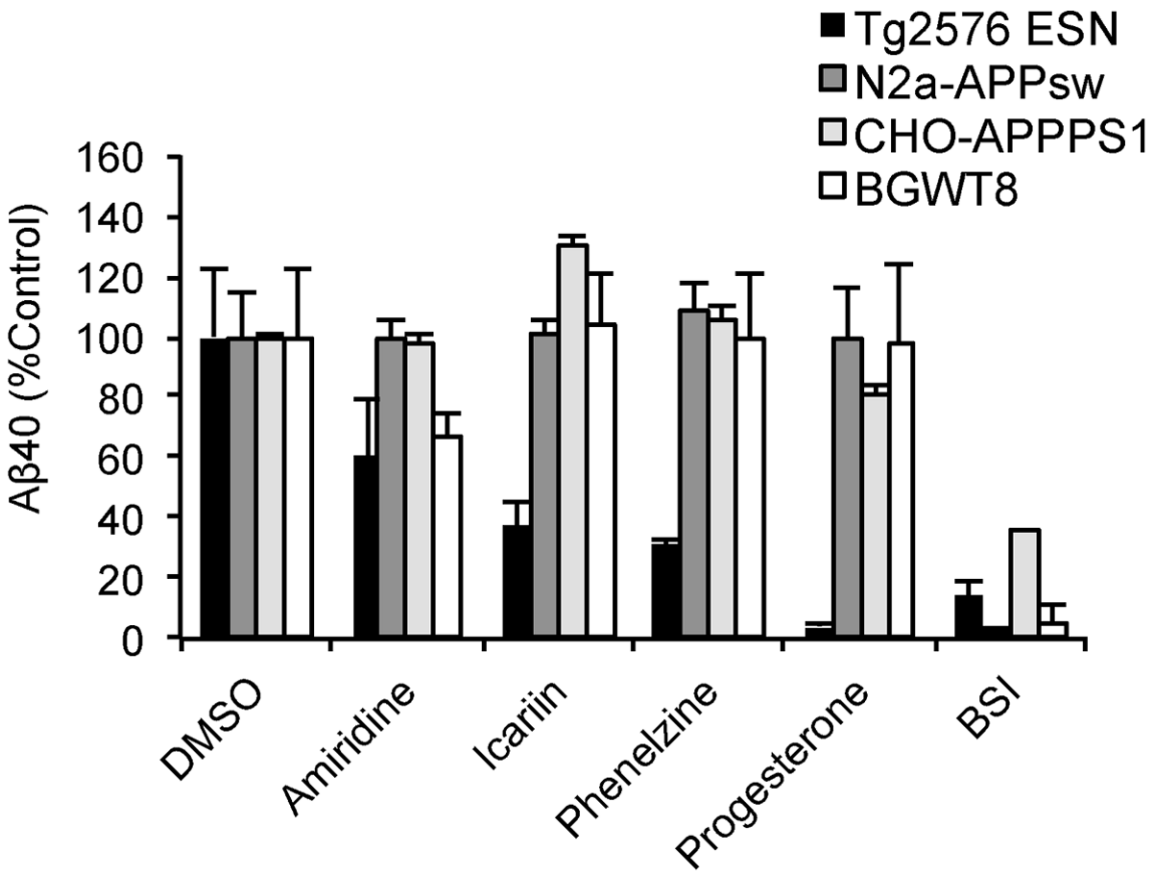

Figure 7. Disparity In Pharmacological Response of Hit Compounds Between Tg2576 ESNs and Cell Lines

(A) Tg2576 ES cell derived neurons; Neuro2a cells stably overexpressing APP_{sw} (N2a-APP_{sw}); Chinese hamster ovary cells stably overexpressing wild type APP and PS1 with the ΔE9 mutation (CHO-APPPS1); and SH-SY5Y cells stably overexpressing GFP-BACE1 and HA-tagged wild type APP (BGWT8) were plated in 96 well plates and treated with hit compounds (10μM) for 6 hours after which media was harvested and tested for Aβ40 content which was normalized to DMSO treated cells for each type (% control). Absolute values for control (DMSO) treated cells are Tg2576 ESNs: 129±29.2 pg/ml; N2a-APP_{sw}: 346±50.7 pg/ml; CHO-APPPS1: 62.5±.7 pg/ml; and BGWT8: 28.8±6.4 pg/ml.